

## Density Functional Study of Crystalline Analogs of Polycarbonates

B. Montanari, P. Ballone,<sup>†</sup> and R. O. Jones\*

Institut für Festkörperforschung, Forschungszentrum Jülich, D-52425 Jülich, Germany

Received May 13, 1998

**ABSTRACT:** Density functional studies have been performed for two crystalline analogs of Bisphenol A polycarbonate (BPA-PC) and for the isolated structural unit. The calculations are free of adjustable parameters and yield equilibrium structures that agree well with available data. Vibrational frequencies have been calculated for the molecular unit. For all structures we have calculated the energy barriers for rotation of segments of the molecule, and we have compared the results with experiment. All phenylene groups rotate freely in the isolated molecular unit, but the corresponding  $\pi$ -flips in the crystalline phases are hindered by the neighboring molecules and reflect the chain packing. The minimum energy barrier for the rotation in the crystal (7.7 kcal/mol) is associated with the rotation of the inner phenylene ring in the molecular unit. The activation energy for the rotation of the methyl groups is 3.4 kcal/mol, independent of the chain packing, and the barriers for rotation of the carbonyl group are 8.7 and 19 kcal/mol in the molecule and crystal phase, respectively.

## I. Introduction

Interest in the family of polycarbonate molecules has grown greatly in the past two decades due to a wide range of industrial applications. Bisphenol A polycarbonate (BPA-PC) is one of the best studied. With excellent optical properties, high impact resistance, and high glass and melting temperatures ( $T_g = 423$  K,  $T_m = 498$  K), its applications range from compact disks to the casings of mobile telephones. Previous work indicates that its strength is related to the motion of localized groups of atoms (such as phenylene rings and carbonyl and methyl groups) and that such motions depend sensitively on the conformation and packing of the chains. A detailed understanding of the microscopic structure of this and related polymers, and how the structure and dynamics influence their macroscopic properties, should assist the development of polymers with tailor-made properties.

Following the work of Williams and Flory<sup>1</sup> thirty years ago, there have been numerous studies of BPA-PC, and its molecular structure has been characterized well by light scattering<sup>2–4</sup> and by diffraction of X-rays<sup>5,6</sup> and neutrons.<sup>7–9</sup> Nuclear magnetic resonance (NMR) has been particularly useful in clarifying the local motion of the chains, and the primary motion detected by this technique is the  $\pi$ -flip of the phenylene groups. References to the extensive literature are provided by Hutnik et al.<sup>10</sup> and Tomaselli et al.<sup>11</sup> Theoretical studies have included static molecular modeling<sup>10,12</sup> and molecular dynamics (MD) calculations using parametrized force fields.<sup>13,14</sup> Quantum mechanical calculations have been performed on fragments of the monomer<sup>15–17</sup> and the results used to generate force fields for the polymer. However, we know of no studies of either monomer or glass that are free of adjustable parameters.

The most precise structural information available on molecules closely related to BPA-PC has come from X-ray diffraction studies on two crystalline forms (re-

ferred to here as C-PC) of the diphenol carbonate of 2,2-bis(4-hydroxyphenyl)propane. The unit cells of these structures contain 118 and 236 atoms, respectively, and the structural unit in both has 59 atoms. In the present work, we describe density functional (DF) calculations on these systems. The DF formalism<sup>18</sup> has provided for decades the most widely used method in condensed matter research that is free of adjustable parameters, and it has acquired acceptance in recent years in applications to molecules and atomic clusters. Combined with molecular dynamics<sup>19</sup> it allows us to simulate the dynamical behavior of systems on the microscopic scale and—as a form of “simulated annealing”—to avoid geometrical structures that correspond to unfavorable local minima in the energy surface.

A major aim of this work is to examine the extent to which the intermolecular interactions influence the motion of chain segments in BPA-PC. The well-defined structures in the crystalline analogues allow one to separate the effects of the intermolecular interactions from those of disorder, and this also motivated the experimental studies. The first form of C-PC was synthesized by Perez and Scaringe,<sup>5</sup> and it was shown by Henrichs and Luss<sup>20</sup> to have a low rate of  $\pi$ -flips of the phenylene rings (the “immobile” form). A second crystal modification was prepared by Henrichs et al.,<sup>6</sup> who showed that the same motion is facile in this “mobile” form.

In previous work<sup>21</sup> we have investigated how different approximations for the exchange-correlation energy describe the intermolecular interaction in the immobile form as well as in crystalline polyethylene (PE). The results indicated that the local spin density (LSD) approximation, derived from the exchange-correlation energy density in a homogeneous, spin-polarized electron gas, overestimates the strength of this interaction. Two modifications based on the gradient of the density were also studied. The BP form—with exchange and correlation contributions due to Becke<sup>22</sup> and Perdew,<sup>23</sup> respectively—underestimates the strength of such bonds (crystalline PE is not bound in such calculations), while use of the form suggested recently by Perdew, Burke, and Ernzerhof (PBE)<sup>24</sup> leads to weak binding in both cases.

\* Corresponding author (e-mail: r.jones@fz-juelich.de).

<sup>†</sup> On leave from Max-Planck-Institut für Festkörperforschung, Heisenbergstr. 1, D-70569 Stuttgart, Germany.

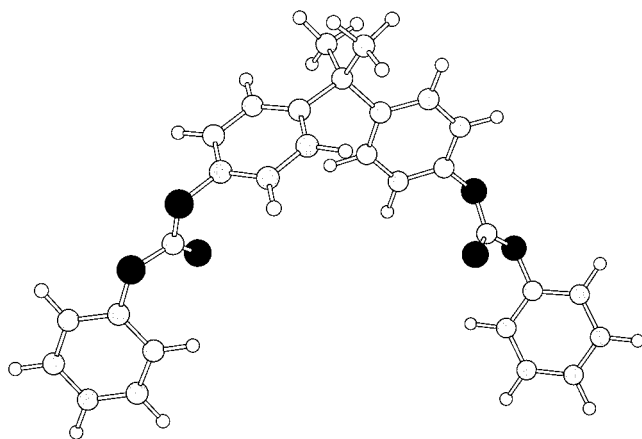


**Figure 1.** Structural units in C-PC. Carbon atoms are gray, oxygen atoms black, and hydrogen atoms white.

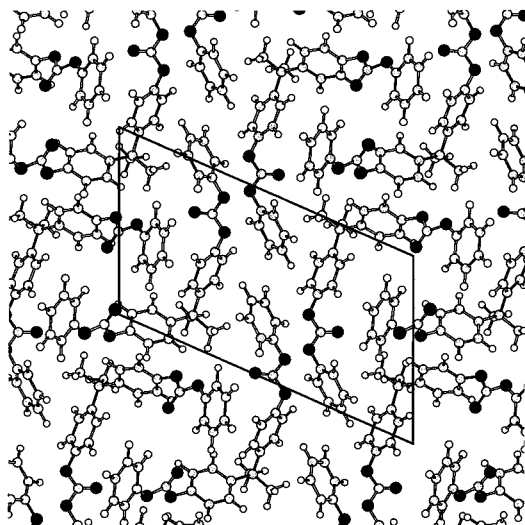
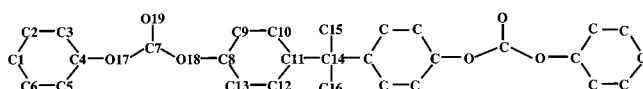


**Figure 2.** Projection of the monoclinic "immobile" structure of C-PC onto the *ac*-plane. Carbon atoms are gray, oxygen atoms black, and hydrogen atoms white.

In this paper we study the structures of the mobile and immobile forms and of the isolated molecular unit shown in Figure 1. We calculate the energy barriers for the  $\pi$ -flip of phenylene rings about their  $C_2$  symmetry axes, the rotation of the methyl groups about the C14–C15 axis (see Chart 1), and the rotation of the

**Chart 1**



$$\Phi_1 = \text{C3-C4-O17-C7}$$

$$\Phi_2 = \text{C7-O18-C8-C9}$$

$$\Psi = \text{C10-C11-C14-C15}$$

carbonyl group about the C7–O17 and O17–O18 axes. Comparison of results obtained under different conditions of interchain packing (or in the absence of neighboring chains) provides insight into the role played by intermolecular interactions in the dynamics of the polymer.

The crystalline structure of the immobile form, with two molecular units per cell, is shown in Figure 2, and the mobile form (four units per cell) is shown in Figure 3. The 59-atom structural units of both structures show

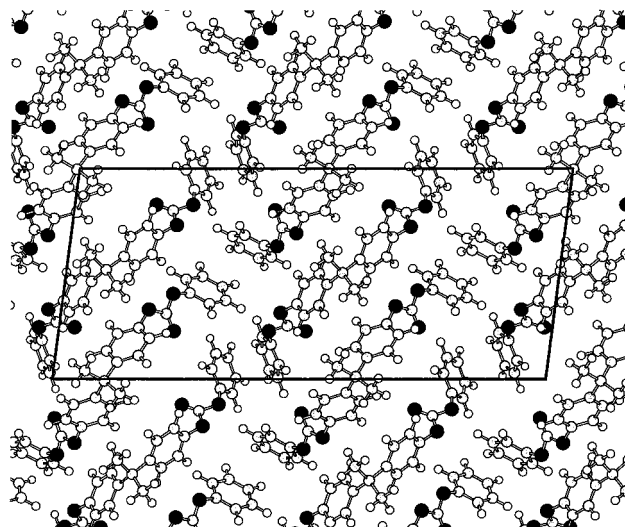


**Figure 3.** Projection of the monoclinic "mobile" structure of C-PC onto the *ac*-plane. Carbon atoms are gray, oxygen atoms black, and hydrogen atoms white.

an extended head-to-tail arrangement reminiscent of the periodic propagation of a linear polymer in the crystalline phase. Essential details of the calculations are provided in Section II. The results for the equilibrium structures and the energy barriers are given in Section III, and we discuss and summarize our findings in Section IV.

## II. Method of Calculation

The method of calculation was described in detail previously.<sup>25,26</sup> The electron–ion interaction is represented by ionic pseudopotentials that have the (nonlocal) form suggested by Troullier and Martins.<sup>27</sup> We use a plane wave basis, and tests showed that reliable energy differences can be obtained for these systems using a kinetic energy cutoff of 35 au. Periodic boundary conditions are assumed. For the single molecular unit we adopt a simple cubic cell with lattice constant 40 au, and the expansion of the orbitals assumes a single point ( $\mathbf{k} = 0$ ) in the Brillouin zone. To minimize systematic errors in comparing the results for the two crystal phases, and to allow more variational freedom in the computation of rotational barriers, we use a simulation cell of 236 atoms for both forms. This corresponds to two unit cells for the immobile form, arranged so that the simulation cell is nearly cubic, and to the experimental unit cell in the mobile form.<sup>6</sup> The volume and shape of the simulation cell were held fixed in all cases.

Our previous calculations<sup>21</sup> indicated that the PBE approximation, which is relatively simple and free of empirical input, is the most reliable in the context of organic molecular crystals. It incorporates an accurate description of the linear response of the uniform electron gas, has the correct behavior under uniform scaling, and results in a smoother potential than in previous approximations. We have used the PBE functional for all systems in the present study, although we shall discuss the relationship to the results of other approximations where relevant.

We have optimized all structures using a combination of DF calculations with MD<sup>28</sup> and a simulated annealing strategy. The calculations were started from the atomic coordinates and unit cells determined from X-ray diffraction data and performed without constraint (on symmetry or otherwise) until the magnitude of the

**Table 1. Selected Interatomic Distances (Å) and Angles (Deg) in the Molecular Unit of C-PC (Scheme 1)<sup>a</sup>**

atoms		atoms	
C4–O17	1.411	C11–C14	1.540
O17–C7	1.365	C14–C15	1.545
O19–C7	1.211	H3–O19	2.494
O18–C7	1.365	H9–O19	3.000
O18–C8	1.415		
C3–C4–O17	123.2	O17–C7–O19	128.0
C5–C4–O17	115.1	C9–C8–O18	121.2
C4–O17–C7	119.2	C13–C8–O18	117.5
C3–C4–O17–C7 ( $\Phi_1$ )	44.8	C9–C8–O18–C7 ( $\Phi_2$ )	69.3
C4–O17–C7–O19	0.0	C10–C11–C14–C15 ( $\Psi$ )	8.4

<sup>a</sup> Hydrogen atoms take the same number as the adjacent C atom.

maximum force on any atom was less than  $5 \times 10^{-4}$  au and the average force on the atoms was 1 order of magnitude less. We emphasize that *all* atomic coordinates are allowed to relax.

The energy barriers for the rotation of the phenylene rings and the carbonyl and methyl groups—both for the condensed phases and the isolated molecule—have been calculated as follows: First, we define a reaction coordinate  $\xi$  (usually an angle) that transforms the initial structure into the rotated one. For selected values of  $\xi$  we then optimize *all* atomic positions, subject only to the constraint  $\xi = \text{constant}$ . The potential energy of the relaxed structure provides information about the rotational barriers, while the structural changes occurring as the barrier is crossed allow us to identify the interactions determining it. The differences between barriers and relaxations found in the isolated molecules and in the condensed phases allow us to distinguish *intra-* from *intermolecular* contributions.

The calculations described here (with the optimization of a structure with 236 atoms in the unit cell) are very demanding of computing resources, particularly as the MD/DF calculations require very large basis sets. The availability of massively parallel computers and the existence of efficient programs mean that even systems of this size can be studied using methods without adjustable parameters.

### III. Results

#### A. Geometrical Structures. 1. Single Molecule.

A detailed analysis of the structural unit (Figure 1, Chart 1) is a prerequisite for understanding the structural and dynamical properties of the condensed phases. We have performed a careful structure optimization of this unit, which has  $C_2$  symmetry in the ground state and report the most important parameters in Table 1. All atomic coordinates are provided as Supporting Information. The aromatic rings have bond angles and lengths that are very close to those of benzene, with minor fluctuations around the average C–C and C–H distances (1.396 and 1.092 Å, respectively). The corresponding distances in benzene—calculated with the same method—are 1.397 and 1.093 Å. The isopropylidene group at the molecular vertex has bond distances and angles close to the ideal  $sp^3$  bonds in hydrocarbons.

The orientation of the phenylene groups and their relationship to the carbonyl group are of central importance. We note first that the C4–O17 bond in the carbonyl group is longer than the C7–O17 bond, although they might appear at first sight to be equivalent. Projection of the DF (Kohn–Sham) orbitals onto atomic

states and the computation of the Mayer bond order show that both bonds have a significant  $\pi$ -character and that this is stronger in C7–O17. The delocalization of the  $\pi$ -electrons is an important contribution to stability<sup>17</sup> and also influences the orientation of the rings. The optimal  $\pi$ -bonding, together with a weak attraction between O19 and the hydrogen of the phenylene rings (see below), would require  $\Phi_1 = \Phi_2 = 0^\circ$ ; the equilibrium angles ( $\Phi_1 = 45^\circ$ ,  $\Phi_2 = 69^\circ$ ) result from a balance between these attractive forces and the short-range repulsion between O19 and H3 and H9.

The difference between  $\Phi_1$  and  $\Phi_2$  is a subtle effect arising from the mutual exclusion of these two hydrogen atoms. The dihedral angles around the O17–C7 and O18–C7 are close to zero, being stiffer and not balanced by steric constraints. The interactions at the carbonyl–phenylene junction lead to angles C3–C4–O17 and C5–C4–O17 that at equilibrium differ significantly from  $120^\circ$ . Computations for deformed configurations show that these two angles depend strongly on the O17–H distance, with short separations being associated with large deviations from  $120^\circ$  in both. These deviations are reduced progressively when the phenylene group is rotated so that the O17–H3 distance increases. Finally, the spatial orientation of the internal rings is determined by the repulsive interaction between the hydrogens in the rings and those in the  $CH_3$  groups (the minimum H–H distance is 2.22 Å).

These results are consistent with earlier work on molecular fragments, with H atoms added to simulate the molecular environment. The bonding within the phenylene, carbonate, and isopropylidene groups is not influenced strongly by intramolecular interactions, and the relative orientation of the groups is determined mainly by steric constraints. Adjacent phenylene and carbonate groups tend to be coplanar, as this favors the delocalization of the  $\pi$ -electrons. These features are reflected in the distribution of the molecular Kohn–Sham eigenvalues (Figure 4), where we also identify the contributions coming from the different bonds. The energy gap to the lowest excited singlet state is 4.4 eV.<sup>29</sup>

The above results allow us to predict the most important dynamical modes in the molecule and in the condensed phases. Rotations of the rings involve only a torsional restoring force and will be facile, with the exception of a narrow range of angles corresponding to close contact between O and H atoms. Rotations of the carbonyl group will be more difficult because of the enhanced  $\pi$ -character of the O17–C7 and O18–C7 bonds. The barriers for methyl group rotations should involve barriers comparable to those observed in saturated hydrocarbons. Since steric interactions between the H in the rings and either O (carbonyl) or H (methyl) are likely to contribute most to the energy barriers, the simultaneous rotation of two groups—avoiding the shortest H–H or O–H distances—should lead to the energetically most favorable path.

These predictions are confirmed by our calculations of the rotational barriers, which are reported in Table 2. Analysis of the relaxed atomic positions for fixed values of the dihedral angles confirm that all barriers are lowered by the simultaneous relaxation of the neighboring groups. The aromatic rings and the carbonate group are nearly planar along the entire path in all cases. The large difference between the barriers for the  $\pi$ -flip of the rings in the isolated molecule and the experimental estimate in the crystal phases (see

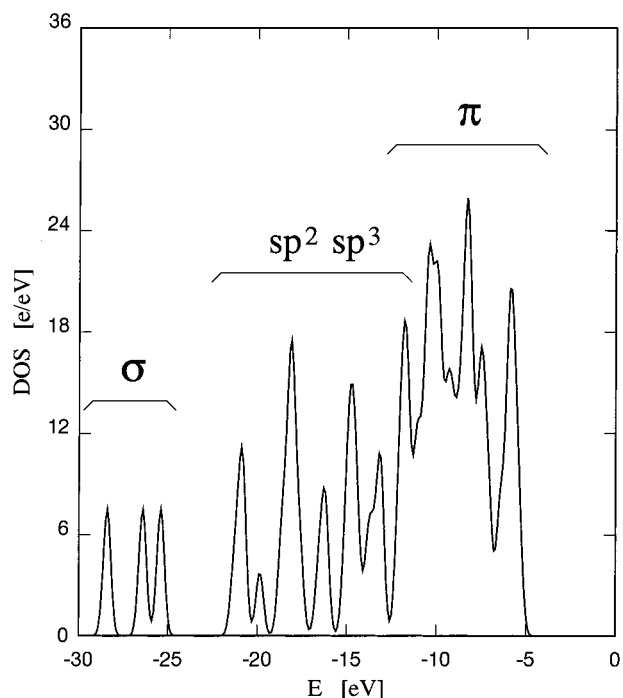


**Figure 4.** Eigenvalues of the density functional (Kohn–Sham) equations for the isolated molecular unit. Each eigenvalue is represented by a Gaussian distribution of width 0.3 eV. The contributions from different bands are also shown.

**Table 2. Rotational Energy Barriers (in kcal/mol) for the Functional Groups of the Isolated Molecular Unit of C-PC<sup>a</sup>**

group	energy barrier	group	energy barrier
methyl	2.86	carbonyl (a)	8.7
int ring	1.98	carbonyl (b)	18.5
ext ring	1.20		

<sup>a</sup> (a), (b) refer to rotations about the C7–O18 and O17–O18 axes, respectively.

next section) shows that the rotational rigidity of the latter arises from intermolecular interactions.

The charge distribution in the molecule has been analyzed in terms of both Mulliken populations and ESP charges, the atomic charges obtained by fitting the electrostatic potential outside the molecule.<sup>30</sup> The electrostatic interactions are localized on the carbonate group and well screened by the neighboring atoms, and the total dipole moment of the molecule (1.0 D)<sup>31</sup> points toward the molecular vertex. The relatively weak electrostatic forces in BPA-PC are also evident in the dielectric constant measured for glassy polycarbonates (3.17),<sup>32</sup> which is typical of weakly ionic organic systems. The effective charges change little if groups are rotated around “easy” axes, and they should provide valuable input for modeling the force field in the molecule.

**2. Crystal Forms.** The structures of the crystalline forms of C-PC have been optimized using the method described in Section II, starting from the experimental coordinates for the mobile<sup>6</sup> and immobile forms.<sup>5</sup> Since existing exchange-correlation energy functionals do not predict quantitatively the equilibrium volume and unit cell of the immobile form,<sup>21</sup> all computations have been performed with the experimental unit cells.

The relaxed atomic positions agree well with the experimental data (a list of all coordinates is provided as Supporting Information): the rms deviations for the coordinates of non-hydrogen atoms of 0.15 and 0.08 Å

**Table 3. Torsional Angles (Deg) Defining the Orientation of the Phenylene Groups in the Molecular Unit and in the Crystal Forms**

	angle	multiplicity	value
molecule	$\Phi_1$	2	45.1
	$\Phi_2$	2	69.2
	$\Psi$	2	8.3
immobile	$\Phi_1$	2	33.3
		2	87.7
	$\Phi_2$	2	88.8
		2	82.0
	$\Psi$	2	36.5
		2	4.4
mobile	$\Phi_1$	4	60.0
		4	49.8
	$\Phi_2$	4	89.0
		4	71.9
	$\Psi$	4	22.4
		4	9.6

for the immobile and mobile forms, respectively, are due mainly to slight rotations of the functional groups, while computed and experimental values for interatomic distances and bending angles are very close. The agreement for the hydrogen coordinates is slightly worse (rms deviations 0.3 and 0.2 Å), although the X-ray determination of the hydrogen positions is less precise. We have studied the effect of using the LSD and BP approximations to the exchange-correlation energy on the calculated structures of the immobile form. The rms deviations for the BP functional are 0.15 and 0.32 Å for the non-hydrogen and hydrogen atoms, respectively. These are very similar to the PBE results, while the corresponding deviations for the LSD functional are greater (0.21 Å, 0.41 Å).

The density is 10% higher in the immobile form than in the mobile form, and we have noted that the molecular arrangements in both mimic the head-to-tail arrangement of glassy polycarbonates. The geometry of the molecular units changes little on forming either crystal, although the relatively soft  $\Phi_1$ ,  $\Phi_2$ , and  $\Psi$  dihedral angles change by up to  $\sim 20^\circ$ . The most pronounced changes are in  $\Phi_1$  and  $\Phi_2$ , which define the orientation of the external ring. With one exception in the immobile form (see Table 3), these angles open up significantly in the crystal, with a related increase in the O19–H3 distance. The corresponding C3–C4–O17 and C5–C4–O17 angles have almost ideal values ( $120^\circ$ ) in the solids, showing that the anomalous values in the molecule are due to the intramolecular O19–H3 bond. The variation in bond lengths with changing volume shows that the intermolecular packing is limited mainly by H–H contacts, with contacts between H and aromatic C atoms playing a secondary role.<sup>33</sup>

The geometrical structures are then described well by DF calculations with the PBE approximation. However, the cohesive energy appears to be underestimated significantly for both crystal forms,<sup>34</sup> and their relative stability (experimentally, the mobile form transforms into the immobile upon annealing) is not reproduced by the calculation. If we calculate the cohesive energy for the optimal PBE structure and add ad hoc attractive pair potentials of the form  $C_{ij}/r$ ,<sup>6</sup> with the  $C_{ij}$  taken from standard potentials for organic molecules, we find a cohesive energy in the correct range<sup>34</sup> and reproduce the higher stability of the immobile form. This indicates that the attractive part of the van der Waals potential is the main feature that is not included in the PBE functional.

The weak structural dependence of the van der Waals forces—they act as a background “glue”, giving rise to cohesion—means that the contribution of short-range repulsive forces is crucial for both structure calculations and developing force fields for polycarbonates. To understand the PBE description of the intermolecular attractions in more detail, we have estimated the electrostatic contribution to cohesion from ESP charges. In both mobile and immobile forms these are  $\sim 0.5$  eV/molecule. We note that the crystal packing is such that the total dipole moment of the unit cell—and the long-range components of the electrostatic interactions—are small in both crystalline forms.

We noted previously<sup>21</sup> that there are numerous weak intermolecular links between hydrogen and either O or C, the presence of which is revealed by short interatomic distances in the ground state and the shrinking of the “bonds” upon homogeneous expansion of the solid. Most of these bonds are between phenylene H atoms and O atoms in neighboring molecules. All require an increase in  $\Phi$  and  $\Psi$  and are formed at the expense of the intramolecular C–H–O groups. There are similar bonds between H atoms and aromatic C atoms. Neither family involves “hydrogen bonds” in the sense of linking two highly electronegative ions, but the basic mechanism is also a weak hydrogen attraction toward electron-rich regions of the system. We estimate that their contribution to cohesion is of the order of 10% of that of the van der Waals forces. We note here that the electronic structure of the molecules changes little on forming the solids, with the DOS being the superposition of the molecular DOS.

**B. Energy Barriers, Dynamical Properties.** We have calculated the energy barriers for the rotation of the methyl and carbonyl groups, as well as for the  $\pi$ -flip of the inner and outer phenylene groups in both forms of C-PC. We discuss first the results for the phenylene rings, because this is the most prominent motion in NMR studies of C-PC.

In the immobile form the outer phenylene group has a rotational barrier of 16.3 kcal/mol. Analysis of the relaxed geometry at the saddle point shows that the intramolecular relaxation is small, while there is a strong coupling with the motion of the *inner* ring in two adjacent molecules: by changing  $\Phi_1$  by  $90^\circ$ ,  $\Phi_2$  and  $\Psi$  on the same molecule change by less than  $3^\circ$ , while the largest values of  $\Delta\Phi_1$ ,  $\Delta\Phi_2$ , and  $\Delta\Psi$  on the two nearest molecules are 7, 31, and  $22^\circ$ , respectively. The relaxation of the inner rings in the neighboring molecules implies a small but definite rotation of one of their methyl groups. The synchronous motion of inner and outer rings in adjacent molecules suggests the existence of a single mechanism for rotating either group in the immobile form; i.e., the barrier to rotate the inner phenylene ring (not computed) should be close to the one computed for the external ring. The 16.3 kcal/mol barrier arises from the short-range repulsion of several H–H pairs (the minimum separations are 1.90 Å at the saddle point and 2.09 Å in the ground state) and the local expansion of intramolecular distances around the rotating phenylene group.

The barrier for the  $\pi$ -flip of the outer ring in the mobile form is 12.6 kcal/mol. The intramolecular relaxation at the saddle point is greater than in the immobile form ( $\Delta\Phi_2 = 13^\circ$ ,  $\Delta\Psi = 26^\circ$  for  $\Delta\Phi_1 = 90^\circ$ ), while weaker intermolecular coupling affects mainly the nearest external phenylene ring in the head-to-tail

arrangement ( $\Delta\Phi_1 = 21^\circ$ ,  $\Delta\Phi_2 = 8^\circ$ , and  $\Delta\Psi = 2^\circ$ ). The relaxation of the inner rings in adjacent molecules is small ( $\sim 3^\circ$ ), and the barrier arises predominantly from local expansion to accommodate the rotating phenylene group. While some H–H distances shrink (the minimum separation is 1.96 Å), most of the interatomic separations increase near the rotating ring.

Finally, rotation of the inner phenylene ring in the mobile form is associated with the smallest energy barrier (7.7 kcal/mol) and relaxation. The strongest couplings are with the propylidene group and the second inner ring in the same molecule ( $\Delta\Psi = 70^\circ$  for the ring whose  $\Phi_2$  changes by  $90^\circ$ ;  $\Delta\Phi_1 = 5^\circ$ ,  $\Delta\Phi_2 = 18^\circ$ , and  $\Delta\Psi = 20^\circ$  for the other half of the same molecular unit). The relaxation most evident in the neighboring units involve one propylidene group ( $\Delta\Psi \sim 10^\circ$  on both sides of the group) with smaller changes ( $\sim 3^\circ$ ) in  $\Phi_1$  and  $\Phi_2$ . In this case there is a small homogeneous expansion around the rotating ring. The previous estimates of the barriers for phenylene ring rotation are 9–10 kcal/mol,<sup>15</sup> 8–9 kcal/mol,<sup>35</sup> 10.4 kcal/mol,<sup>10</sup> and 9.6 kcal/mol.<sup>36</sup> Our results agree satisfactorily with experiment and allow us to identify the mobile group observed as the inner phenylene group. A molecular dynamics simulation for BPA-PC led to a higher value (12.6 kcal/mol).<sup>14</sup>

The barrier associated with the rotation of the methyl group is  $\sim 3.4$  kcal/mol in both crystalline forms and  $\sim 2.9$  kcal/mol in the isolated molecular unit. It is almost independent of the chain packing, and our analysis shows that it is determined primarily by intramolecular interactions. An earlier semiempirical estimate of this barrier was 6.6 kcal/mol.<sup>15</sup>

The rotation of the carbonyl around the O18–C7 axis has been discussed for the isolated structural unit. This would require substantial intermolecular relaxation in the condensed phases, and the lowest energy path in the crystals is found to be the rotation around the O17–O18 axis. This barrier (19 kcal/mol) is nevertheless close to the molecular barrier and is due mainly to intramolecular interactions. The reorientation of the external phenylene ring observed implies a small relaxation in the external ring of the neighboring molecule.

**C. Vibration Frequencies of the Structural Unit.** The vibrational eigenvalues and eigenvectors for the molecular unit have been calculated using a finite difference approximation for the dynamical matrix. The results are provided as Supporting Information. While anharmonic effects limit the accuracy of the computation, especially for the lowest frequencies ( $\omega \leq 300$   $\text{cm}^{-1}$ ), the results reported in Figure 5 provide new information about this molecule. We show the vibrational density of the infrared active states and—in the inset—the density of states of all modes. These data should be useful in refining the parameters of force field models.

The infrared active modes involve mainly vibrations of the carbonate group, the most ionic part of the molecule. The peaks at 725 and 1139  $\text{cm}^{-1}$  are “out of plane” and “in-plane” bending modes, respectively, of this group. The bending mode for the C8–O18–C7 angle is at 1580  $\text{cm}^{-1}$ , and the stretching of the carbonyl group is at 1774  $\text{cm}^{-1}$ . The peak at 3135  $\text{cm}^{-1}$  arises from stretching modes of the (aromatic C)–H bonds. These results are in good agreement with the measured infrared spectra.<sup>37</sup> On the basis of symmetry we find that Raman activity is allowed for modes localized on

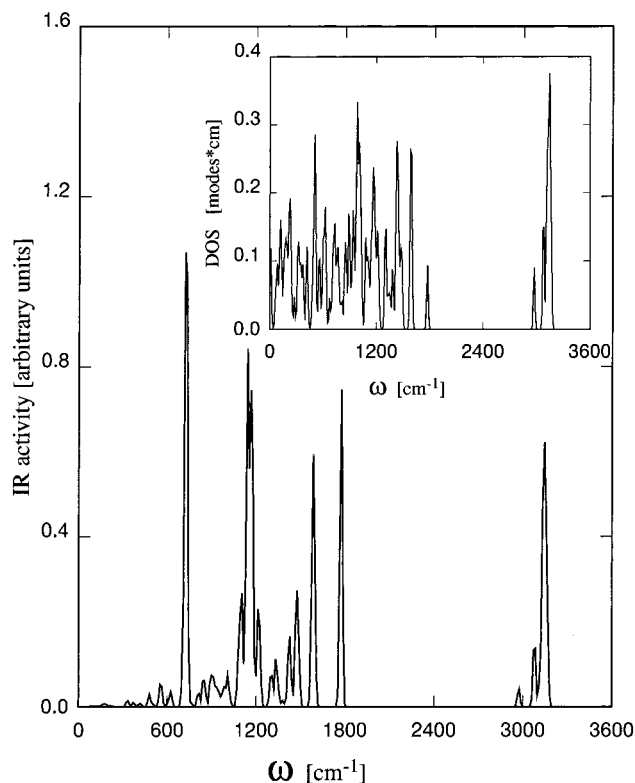


**Figure 5.** Infrared active vibrational spectrum of the isolated molecular unit. The inset shows the total vibrational density of states. Each mode is represented by a Gaussian distribution of width  $12\text{ cm}^{-1}$ .

the carbonate group, the isopropylidene unit ( $1217$  and  $3078\text{ cm}^{-1}$ ), and on the phenylene groups ( $1471$  and  $1586\text{ cm}^{-1}$ ).

We now turn to the total vibration spectrum, discussing the modes in the order of decreasing frequency. The highest frequencies arise from stretching modes of the aromatic C–H bonds ( $3110$ – $3166\text{ cm}^{-1}$ ), and a smaller band of the  $\text{sp}^3$  C–H bond stretching (at  $2970$  and  $3070\text{ cm}^{-1}$ ). The carbonyl stretching near  $1770\text{ cm}^{-1}$  is followed by a wide band ( $1470$ – $1600\text{ cm}^{-1}$ ) of stretching modes of the carbon backbone. Carbon stretching is mixed with C–H bond bending at lower frequencies, and the stretching of the carbon–tetrahedral oxygen occurs at  $1210\text{ cm}^{-1}$ . There are bending modes between  $1010$  and  $1200\text{ cm}^{-1}$  that preserve the planarity of the benzene and carbonate ( $-\text{O}-\text{C}-\text{O}-$ ) groups. The out-of-plane vibrations of these groups follow between  $400$  and  $1000\text{ cm}^{-1}$ . About 30 low-frequency modes cannot be identified reliably by our calculation, but this frequency range covers the rotations and librations of the constituent groups.

#### IV. Concluding Remarks

We have calculated the optimum structure of two crystalline modifications (referred to as the “mobile” and “immobile” forms of C-PC) of Bisphenol A polycarbonate (BPA-PC), as well as for the isolated structural unit of both. If the unit cell is constrained to have the experimental dimensions, density functional calculations reproduce the measured structures very well, and the structure of the individual molecular units are affected little by the presence of the surrounding molecules in the crystalline phases. Some dihedral angles are modified slightly by the intermolecular interactions, and this can be attributed to the relatively

low force constants associated with these torsional degrees of freedom. We have observed the presence of unusual hydrogen bonds between molecules in the crystals that contribute to cohesion in the crystalline forms.

For the mobile and immobile structures and for the isolated molecular unit we have calculated energy barriers for the motion of several molecular groups: (a) the  $\pi$ -flip of the phenylene rings about their  $C_2$  symmetry axes; (b) the rotation of the methyl group about the C14–C15 axis (see Chart 1); (c) the rotation of the carbonyl group about the C7–O17 and O17–O18 axes. We have found:

- The phenylene rings rotate freely in the isolated molecular units. The presence of surrounding molecules hinders the rotation in the crystalline phases by amounts that depend strongly on the crystal packing.

- In agreement with experiment, we find two mechanisms for the  $\pi$ -flips of the phenylene rings in the mobile form. The smaller energy barrier is associated with the motion of the inner ring, and its value ( $7.7\text{ kcal/mol}$ ) is in good agreement with experimental estimates. We identify the measured barrier as arising from the motion of this ring.

- The barrier associated with the rotation of the methyl group is  $3.4\text{ kcal/mol}$ , independent of the chain packing.

- The rotation of the carbonyl group around the O17–O18 axis requires an energy of  $19\text{ kcal/mol}$ . As in the case of the methyl group, this barrier is determined mainly by intramolecular interactions and depends only weakly on the chain packing.

We emphasize again that we optimize *all* atomic positions in the unit cell, so that the interrelationships between the motions of different groups in the systems can be observed. Computations on systems with a relatively small number of atoms cannot account for long-range relaxations and the release of elastic energy. Nevertheless, the good agreement with the experimental data indicates that such effects are of secondary importance.

Together with earlier results on related systems, the present work shows that density functional calculations provide reliable data on the energy surfaces of organic molecules and molecular solids. The geometries, energy surfaces, and vibrational frequencies so obtained are being used to refine the parametrizations of force fields for use in large scale Monte Carlo and molecular dynamics calculations for these and related systems.

**Acknowledgment.** The calculations were performed on the Cray T3E-600/512 and T3E-900/256 computers in the Forschungszentrum Jülich with grants of CPU time from the Forschungszentrum and the German Supercomputer Centre (HLRZ). The work is supported by the MaTech Program (03N8008E0) of the Bundesminister für Bildung, Wissenschaft, Forschung und Technologie, Bonn. We thank H. Hesse, U. W. Suter, and participants in this program for helpful discussions.

**Supporting Information Available:** Tables of atomic coordinates, vibration frequencies, and eigenvectors are available in electronic form. See any current masthead page for accessing instructions.

#### References and Notes

- (1) Williams, A. D.; Flory, P. J. *J. Polym. Sci., Polym. Phys. Ed.* **1968**, *6*, 1945.

- (2) Erman, B.; Marvin, D. C.; Irvine, P. A.; Flory, P. J. *Macromolecules* **1982**, *15*, 664.
- (3) Erman, B.; Wu, D.; Irvine, P. A.; Marvin, D. C.; Flory, P. J. *Macromolecules*, **1982**, *15*, 670.
- (4) Floudas, G.; Lappas, A.; Fytas, G.; Meier, G. *Macromolecules* **1990**, *23*, 1747.
- (5) Perez, S.; Scaringe, R. P. *Macromolecules* **1987**, *20*, 68.
- (6) Henrichs, P. M.; Luss, R. H.; Scaringe, R. P. *Macromolecules* **1989**, *22*, 2731.
- (7) Cervinka, L.; Fischer, E. W.; Hahn, K.; Jiang, B.-Z.; Hellmann, G. P.; Kuhn, K. J. *Polymer* **1987**, *28*, 1287.
- (8) Cervinka, L.; Fischer, E. W.; Dettenmaier, M. *Polymer* **1991**, *32*, 12.
- (9) Floudas, G.; Higgins, J. S.; Meier, G.; Kremer, F.; Fischer, E. W. *Macromolecules* **1993**, *26*, 1676.
- (10) Hutnik, M.; Argon, A. S.; Suter, U. W. *Macromolecules* **1991**, *24*, 5970.
- (11) Tomaselli, M.; Robyr, P.; Meier, B. H.; Grob-Pisano, C.; Ernst, R. R.; Suter, U. W. *Macromolecules* **1996**, *29*, 1663.
- (12) Hutnik, M.; Gentile, F. T.; Ludovice, P. J.; Suter, U. W.; Argon, A. S. *Macromolecules* **1991**, *24*, 5962.
- (13) Shih, J. H.; Chen, C. L. *Macromolecules* **1995**, *28*, 4509.
- (14) Fan, C. F.; Cagin, T.; Shi, W.; Smith, K. A. *Macromol. Theory Simul.* **1997**, *6*, 83. See also: Fan, C. F.; Cagin, T.; Chen, Z. M.; Smith, K. A. *Macromolecules* **1994**, *27*, 2383.
- (15) Bicerano, J.; Clark, H. A. *Macromolecules* **1988**, *21*, 585 [semiempirical calculations].
- (16) Laskowski, B. C.; Yoon, D. Y.; McLean, D.; Yaffe, R. L. *Macromolecules* **1988**, *21*, 1629 [Hartree-Fock calculations on diphenyl carbonate and diphenylpropane].
- (17) Sun, H.; Mumby, S. J.; Maple, J. R.; Hagler, A. T. *J. Phys. Chem.* **1995**, *99*, 5873 [Hartree-Fock, Møller-Plesset, and density functional calculations of carbonic acids, methyl and dimethyl carbonates, phenyl carbonates, and 2,2-diphenylpropane]. See also: Sun, H.; Mumby, S. J.; Maple, J. R.; Hagler, A. T. *J. Am. Chem. Soc.* **1994**, *116*, 2978.
- (18) See, for example: Jones, R. O.; Gunnarsson, O. *Rev. Mod. Phys.* **1989**, *61*, 689. *Density Functional Theory*; NATO ASI Series, Series B, Physics; Vol. 337; Gross, E. K. U., Dreizler, R. M., Eds.; Plenum: New York, 1995.
- (19) Car, R.; Parrinello, M. *Phys. Rev. Lett.* **1985**, *55*, 2471.
- (20) Henrichs, P. M.; Luss, H. R. *Macromolecules* **1988**, *21*, 860.
- (21) Montanari, B.; Ballone, P.; Jones, R. O. *J. Chem. Phys.* **1998**, *108*, 6947 and references therein.
- (22) Becke, A. D. *Phys. Rev. A* **1988**, *38*, 3098.
- (23) Perdew, J. P. *Phys. Rev. B* **1986**, *33*, 8822.
- (24) Perdew, J. P.; Burke, K.; Ernzerhof, M. *Phys. Rev. Lett.* **1996**, *77*, 3865.
- (25) Borrmann, A.; Montanari, B.; Jones, R. O. *J. Chem. Phys.* **1997**, *106*, 8545.
- (26) Montanari, B.; Jones, R. O. *Chem. Phys. Lett.* **1997**, *272*, 347.
- (27) Troullier, N.; Martins, J. M. *Phys. Rev. B* **1991**, *43*, 1993.
- (28) CPMD program version 3.0, Hutter, J. et al., Max-Planck-Institut für Festkörperforschung and IBM Research 1990-98.
- (29) The gap has been computed as the difference in total energy between the ground state and the state with an additional electron ( $\Delta$ SCF calculation). The difference between the eigenvalues of the highest occupied and lowest unoccupied states in LSD calculations usually underestimates this quantity.
- (30) Singh, U. C.; Kollman, P. A. *J. Comput. Chem.* **1984**, *4*, 129-145. Chirlian, L. E.; Francl, M. M. *J. Comput. Chem.* **1987**, *8*, 894-905. Besler, B. H.; Merz, K. M.; Kollman, P. A. *J. Comput. Chem.* **1990**, *11*, 431-439. Breneman, C. M.; Wiberg, K. B. *J. Comput. Chem.* **1990**, *11*, 361-373.
- (31) This is a revision of the value given in ref 21.
- (32) Brydson, J. A. *Plastics Materials*; Butterworth: London, 1982; p 511.
- (33) The shortest intermolecular H-H distances are 2.09 and 2.32 Å in the immobile and mobile forms, respectively. The corresponding values for the shortest C-H distance are 2.60 and 2.79 Å.
- (34) We know of no experimental data on the low-temperature cohesive energy of C-PC. Comparison with data for glassy polycarbonates suggests a cohesive energy of  $\sim 2$  eV per molecular unit. See, for example: Gentile, F. T.; Suter, U. W. In *Materials Science and Technology*; Cahn, R. W., Haasen, P., Kramer, E. J., Eds.; VCH: Weinheim, 1993; Vol. 12, p 33 (see p 57).
- (35) Henrichs, P. M.; Nicely, V. A. *Macromolecules* **1991**, *24*, 2506.
- (36) Walton, J. H.; Lizak, M. J.; Conradi, M. S.; Gullion, T.; Schaefer, J. *Macromolecules* **1990**, *23*, 416.
- (37) Schmidt, P.; Dybal, J.; Turska, E.; Kulczycki, A. *Polymer* **1991**, *32*, 1862.

MA980770J